# Effective Optimization of the Control System for the Cement Raw Meal Mixing Process: Simulating the Effect of the Process Parameters on the Product Homogeneity

DIMITRIS TSAMATSOULIS
Halyps Building Materials S.A., Italcementi Group
17th Klm Nat. Rd. Athens – Korinth
GREECE
d.tsamatsoulis@halyps.gr http://www.halyps.gr

*Abstract:* - The main factors that influence the quality of the raw meal during its production in a ball mill and storage in stock and homogenisation silos of continuous flow are investigated. A detailed simulation is used, incorporating all the key characteristics of the processes. The quality modules of the raw meal are controlled via robust PID controllers, optimized with the same simulator. The effect of the qualitative consistency of the raw materials, of the active volume of the material contained in the silos, of the stock silo filling degree, of the sampling period and of the time needed for preparation and analysis is quantified. The developed simulator, not only can be applied to obtain the optimum PID parameters among the sets satisfying certain robustness criteria, but also to determine optimum conditions of the process parameters.

*Key-Words:* - Dynamics**,** Raw meal, Quality, Mill, Model, Variance, PID, Robustness, Homogeneity

## 1 Introduction

In cement industry a huge amount of efforts in process control have been dedicated on raw meal homogeneity as it is the main factor influencing the clinker activity [1]. Primarily the control is performed in the mill by adjusting the weight feeders according to the raw meal chemical modules in the mill (RM) outlet. The regulation is mainly obtained via PID [2, 3] and adaptive controllers [4, 5, 6, 7].

As clearly Kural et al. [5] declare, the disturbances coming from the variations in the chemical compositions of the raw materials from long-term average compositions cause the changes of the system parameters. Tsamatsoulis [8] built a reliable model of the dynamics among the chemical modules in the outlet of an actual raw meal grinding installation and the proportion of the raw materials. The flow chart of the investigated closed circuit process is shown in Figure 1 of [8], including three raw materials feeders. The mill exit stream is fed to a homogenizing silo connected in series with a bigger storage silo. From the stock silo, the raw meal is directed to the kiln inlet. An analytical simulation of the blending process was developed in [3] aiming at optimizing installed PID controllers. The controllers regulate the Lime Saturation Factor (LSF) and Silica Module (SM) in RM outlet, acting on the feeders of limestone and additives. Conventional data were utilized, as concerns the process and raw materials, representing the regular operation of the installation under examination. The classical PID controllers were tuned according to the M - Constrained Integral Gain Optimization (MIGO) method [9]. The simulation led in some optimum PID coefficients for the given settings of the process and raw materials.

The objective of the present analysis is to apply the mentioned simulation in order to investigate the impact of the process parameters on the raw meal stability as concerns its quality. The simulator operates always in automatic mode and a search for the optimum PID parameters is performed if needed. A similar approach to optimize a fuzzy controller for cement raw material blending is applied from Bavdaz et al. [10]. In this case the control algorithm was tested on the raw mill simulation model within a Matlab™, Simulink™ environment. Therefore the present study can be considered as an application of the special attention that is paid to the problems of the synthesis of complex systems' dynamical models, to the construction of efficient control models, and to the development of simulation [11].

## 2 Process Model

### 2.1 Proportioning Modules Definition

For the main oxides contained in the cement semifinal and final products, the following abbreviations are commonly used in the cement industry: C=CaO, S=$SiO_2$, A=$Al_2O_3$, F=$Fe_2O_3$. Three proportioning modules are used to indicate the quality of the raw meal and clinker. [1]:

*Lime Saturation Factor*

$$LSF = \frac{100 \cdot C}{2.8 \cdot S + 1.18 \cdot A + 0.65 \cdot F} \quad (1)$$

$$Silica\ Modulus \quad SM = \frac{S}{A + F} \quad (2)$$

$$Alumina\ Modulus \quad AM = \frac{A}{F} \quad (3)$$

The regulation of some or all of the indicators (1) to (3) contributes drastically to the achievement of a stable clinker quality.

## 2.2 Block Diagram and Transfer Functions

The block diagram shown in Figure 1 and the respective transfer functions are presented in [3] and repeated here for elucidation reasons.

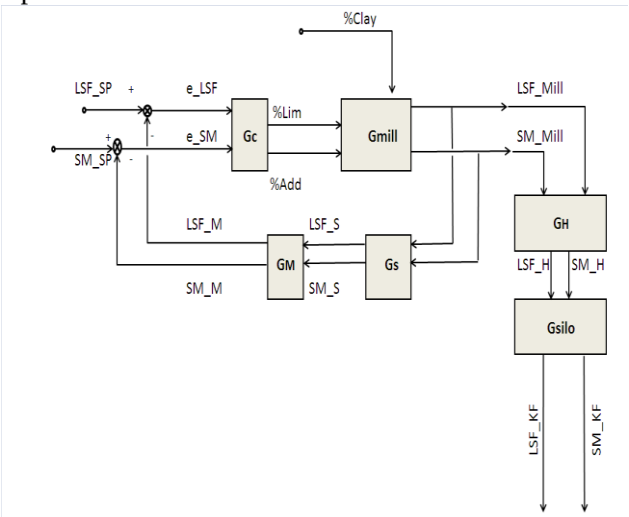


Figure 1. Block diagram of the grinding and blending process.

Where $G_c$ indicates the transfer function of the controller. With $G_{mill}$, the RM transfer function is symbolized, containing three separate functions. The raw meal sampling in the RM outlet is performed via a sampling device, accumulating an average sample during the sampling period. The integrating action of the sampler is denoted by the function $G_s$. The delay caused by the sample transfer, preparation and analysis is shown by the function $G_M$. The raw meal is homogenized in overflow silo with transfer function $G_H$. Then the raw meal before to enter to the kiln is stocked to a storage silo with transfer function $G_{silo}$.

%Lim, %Add, %Clay = the weight percentages of the limestone, additives and clay in the three feeders. In the clay feeder a mixture Limestone: Clay = 0.5 is put. $LSF_{Mill}$, $SM_{Mill}$ = the spot values of LSF and SM in the RM outlet, while $LSF_S$, $SM_S$, $LSF_M$, $SM_M$ = the modules of the average sample and the measured one. Finally $LSF_H$, $SM_H$, $LSF_{KF}$, $SM_{KF}$ = the corresponding modules in the homo silo outlet and in the kiln feed. The LSF and SM set points are indicated by $LSF_{SP}$ and $SM_{SP}$ respectively, while e_LSF and e_SM stand for the error between set point and respective measured module.

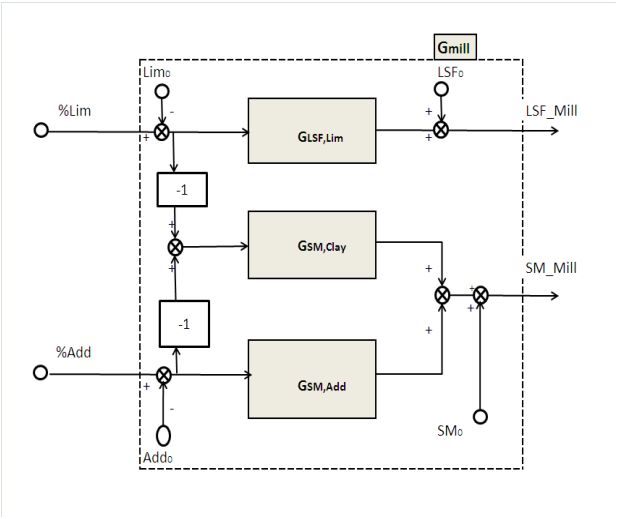


Figure 2. Transfer functions of the RM block.

The raw meal mixing in the RM installation is analyzed in more detail in Figure 2.The functions between the modules and the respecting percentages of the raw materials are indicated by $G_{LSF,Lim}$, $G_{SM,Clay}$, $G_{SM,Add}$. The $G_M$ and $G_s$ functions are described by equations (4) and (5) respectively:

$$G_M = e^{-tM \cdot s} \quad (4)$$

$$G_s = \frac{1}{T_s \cdot s}(1 - e^{-Ts \cdot s}) \quad (5)$$

Based on previous results [2, 8] a second order with time delay (SOTD) model is chosen for each of the functions $G_{LSF,Lim}$, $G_{SM,Clay}$, $G_{SM,Add}$ described by the equation (6):

$$G_x = \frac{k_{g,x}}{(1 + T_{0,x} \cdot s)^2} \cdot e^{-td,x \cdot s} \quad (6)$$

Where x = Lim, Clay or Add. The $k_g$, $T_0$, $t_d$ parameters symbolize the gain, the time constant and the time delay respectively. To avoid elevated degrees of freedom the following equalities are considered:

$$T_{0,Clay} = T_{0,Add} \quad t_{d,Clay} = t_{d,Add} \quad (7)$$

The homo and stock silo transfer functions are given by the first order equations (8) and (9) respectively:

$$G_H = \frac{y_H}{y_{H,In}} = \frac{1}{1 + T_H \cdot s} \quad (8)$$

$$G_{Silo} = \frac{y_{KF}}{y_H} = \frac{1}{1 + T_{Silo} \cdot s} \quad (9)$$

Where $y_H$=$LSF_H$ or $SM_H$, $y_{H,In}$=$LSF_{H,In}$ or $SM_{H,In}$, $y_{KF}$=$LSF_{KF}$ or $SM_{KF}$. $T_H$ and $T_{Silo}$ represent the homo and stock silo first order time constants.

The model parameters are evaluated in [3] using hourly data of feeders' percentages and proportioning modules of a period covering enough months. The procedure to estimate the mean parameters of the raw mill dynamics and their uncertainty as well is analytically described in [8]. The dynamical parameters values are depicted in Table 1.

Table 1. Average and standard deviation of the model parameters

| | Average | Standard Dev. |
|---|---|---|
| $K_{g,Lim}$ | 2.96 | 0.82 |
| $T_{0,Lim}$(h) | 0.19 | 0.15 |
| $t_{d,Lim}$(h) | 0.41 | 0.13 |
| $K_{g,Clay}$ | 0.036 | 0.030 |
| $K_{g,Add}$ | 0.437 | 0.291 |
| $T_{0,Add}$(h) | 0.33 | 0.18 |
| $t_{d,Add}$(h) | 0.33 | 0.18 |

The time constants of the homo and stock silos transfer functions are found using the AM module silos' input and output. As the homo silo operates with overflow, it is always considered to be full. As to the stock silo, the empty meters during the operation are also taken into account. The processing of one full year data provided the following results:

$$T_H = 3.0 \pm 0.6\ h$$

$$T_{Silo} = 16.3 \cdot H_E^{-0.6} \pm 1.3\ h \quad (10)$$

Where $H_E$= the empty meters of the stock silo. To notice that each meter of the stock contains 330 tons of raw meal.

## 2.3 PID Controllers

LSF and SM modules are regulated using two independent PID controllers. Thus the TITO process is simplified to two SISO processes. The controllers are described by equation (11) in Laplace form:

$$\frac{u}{e} = k_p + \frac{k_i}{s} + k_d s \quad (11)$$

The variables $k_p$, $k_i$, $k_d$ represent the proportional, integral and differential gains of the controller. The other variables have the following meaning: e = $LSF_{SP}$-$LSF_M$ or $SM_{SP}$-$SM_M$, u = %Lim or %Add, ($k_p$,$k_i$,$k_d$) = ($k_{pLSF}$,$k_{iLSF}$,$k_{dLSF}$) or ($k_{pSM}$,$k_{iSM}$,$k_{dSM}$).This equation is expressed by function (12) in discrete time domain, where as time interval, the sampling period is considered.

$$u_n = u_{n-1} + k_p \cdot (e_n - e_{n-1}) + T_s \cdot k_i \cdot e_n + k_d \cdot \frac{1}{T_s} \cdot (e_n + e_{n-2} - 2 \cdot e_{n-1}) \quad (12)$$

The integral and differential times $T_i$ and $T_d$ are connected with the respective gains by equation (13).

$$k_i = {k_p}/{T_i}\ ,\ k_d = k_p \cdot T_d \quad (13)$$

The PID sets for the two controllers are selected among the computed ones in [3] for the same RM circuit by implementing the MIGO technique. As robustness criterion in this previous analysis the Maximum Sensitivity was considered provided by equation (14):

$$M_s = Max(|S(i\omega)|) \quad (14)$$

The $k_p$, $k_i$ values as function of $k_d$ and $M_s$ for the two controllers are shown to Figures 3 to 6.

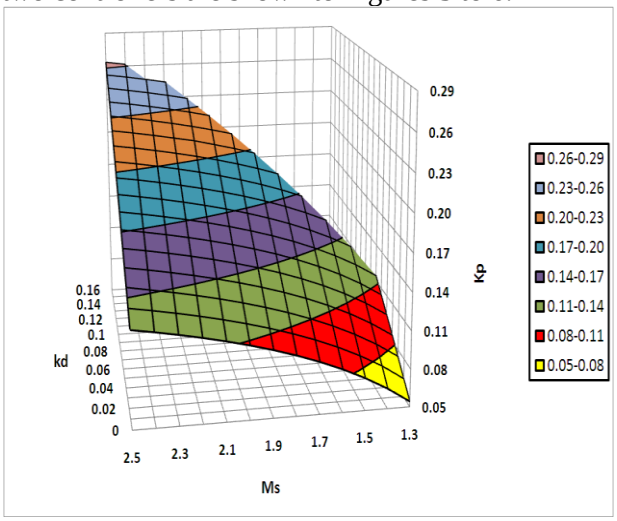


Figure 3. LSF controller. $K_p$ as function of $k_d$, $M_s$.

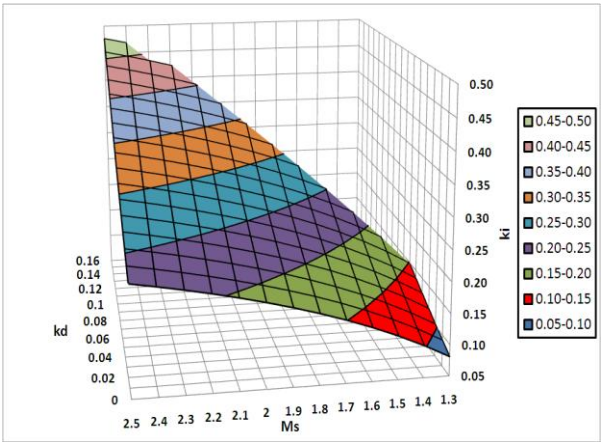


Figure 4. LSF controller. $K_i$ as function of $k_d$, $M_s$.

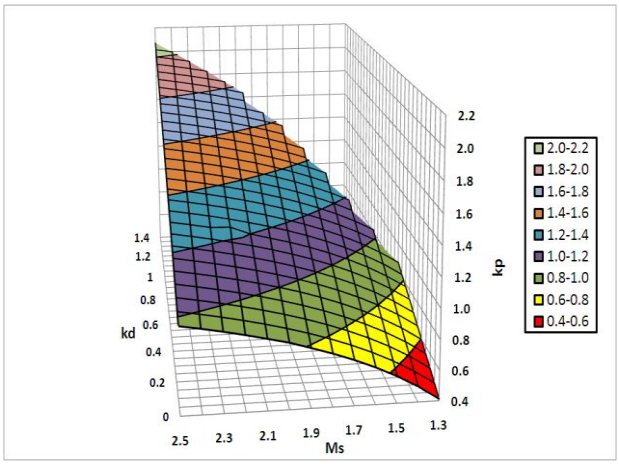


Figure 5. SM controller. $K_p$ as function of $k_d$, $M_s$.

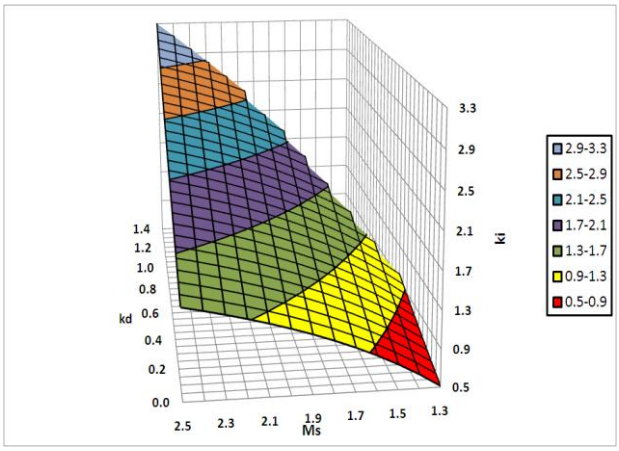


Figure 6. SM controller. $K_i$ as function of $k_d$, $M_s$.

## 2.4 Simulator Basic Data Set

The developed simulator is analytically described in [3]. The steps of its implementation were also enumerated. The raw materials composition based on processing of routine analysis data and used in the simulation is shown in Table 2. The basic data set of process parameters is also indicated in Table 3.

Table 2. Raw materials analysis

| | Limestone | | Clay | |
|---|---|---|---|---|
| Oxide | Aver. | Std. Dev. | Aver. | Std. Dev. |
| $SiO_2$ | 1.25 | 0.35 | 43.32 | 4.80 |
| $Al_2O_3$ | 0.50 | 0.12 | 7.52 | 1.08 |
| $Fe_2O_3$ | 0.29 | 0.07 | 3.98 | 0.51 |
| CaO | 54.18 | 0.67 | 20.79 | 3.82 |
| %Moist. | 3.4 | 1.2 | 10.2 | 1.7 |
| N | 31 | | 112 | |
| LSF | 1266 | | 15.7 | |
| | Average | | Std. Dev. | |
| Lim./ Clay | 0.5 | | 0.1 | |
| Oxide | Iron Oxide | | Bauxite | |
| $SiO_2$ | 1.0 | | 4.1 | |
| $Al_2O_3$ | 0.5 | | 38.9 | |
| $Fe_2O_3$ | 95.0 | | 8.5 | |
| CaO | 1.0 | | 20.6 | |
| Baux /Iron | 3.0 | | | |

Table 3. Simulation data

| | | |
|---|---|---|
| Total RM Run Time (h) | 100 | |
| Constant Composition | Limestone | Clay |
| Min. Time (h) | 4 | 4 |
| Max. Time (h) | 16 | 16 |
| Period of Constant RM Dynamics | | |
| Min. Time (h) | 8 | |
| Max. Time (h) | 20 | |
| Sampling Measurement Delay Time (min) | 20 | |
| Volume Ratios | Average | Std. Dev |
| Lim. / Clay | 0.5 | 0.1 |
| Baux./ Iron | 3.0 | |
| RM LSF Dynamics | | |
| $T_0$ (h) | 0.19 | 0.15 |
| $t_d$ (h) | 0.41 | 0.13 |
| RM SM Dynamics | | |
| $T_0$ (h) | 0.33 | 0.18 |
| $t_d$ (h) | 0.33 | 0.18 |
| Sampling Period (h) | 1.0 | |
| LSF Target | 97.6 | |
| SM Target | 2.5 | |
| Sample Preparation and XRF Reproducibility | | |
| LSF | 0.69 | |
| SM | 0.018 | |
| Initial Feeding Feeders' Settings | | |
| Limestone | 0.5 | |
| Iron | 0.02 | |
| Mill Dry Production | 145 | |
| Electro-filter Flow Rate | 8 | |
| Kiln Feed Flow Rate | 125 | |

Table 3. Cont.

| Filter Oxides | Average | Std. Dev |
|---|---|---|
| $SiO_2$ | 9.87 | 0.49 |
| $Al_2O_3$ | 4.05 | 0.14 |
| $Fe_2O_3$ | 2.25 | 0.09 |
| CaO | 43.63 | 0.15 |
| Homo Active Quantity (tn) | 428 | 92 |
| Stock Time Const. $=16.3 \cdot Empt\_Met^{-0.602} \pm 1.3$ h | | |
| Initial Homo and Stock Compositions | | |
| $SiO_2$ | 13.92 | |
| $Al_2O_3$ | 3.34 | |
| $Fe_2O_3$ | 2.23 | |
| CaO | 42.58 | |
| Stock Silo tn/m | 330 | |
| | Min. | Max. |
| Start up empty meters | 4.0 | 6.0 |
| Empty to Stop RM (m) | 3 | |
| Empty to Start RM (m) | 5 | |

# 3 Effect of the Process Parameters on the Chemical Modules Variance

## 3.1 Uncertainty of the Raw Materials Composition

To study the impact of the uncertainty magnitude of the raw materials' composition on the LSF and SM variance the simulator is applied as follows:

(a) The basic data presented in Tables 2 and 3 are considered.

(b) The standard deviation of the clay's four oxides is modified using the formula:

$$s_{ox} = \alpha \cdot s_{ox,Init} \quad (15)$$

Where ox = C, S, A, F and with the subscript "Init" the standard deviations shown in Table 2 are denoted. The coefficient α is varied from 0.4 to 1.6 with a step of 0.2

(c) The time period with constant clays' composition in the basic Table 3 is between 4 and 16 hours resulting in an average period $T_{cc}$= 10 ± 6 hours. This period is varied from 10 ± 6 to 24 ± 6 hours with a step of 2 hours.

(d) The subsequent controllers' settings are utilized:
LSF: $M_s$=1.5, ($k_p$, $k_i$, $k_d$) = (0.152, 0.219, 0.08)
SM: $M_s$=1.5, ($k_p$, $k_i$, $k_d$) = (1.18, 1.48, 0.7)

The results of the two modules standard deviation in RM outlet as function of the clays' variance and period of constant composition are depicted in Figures 7, 8.

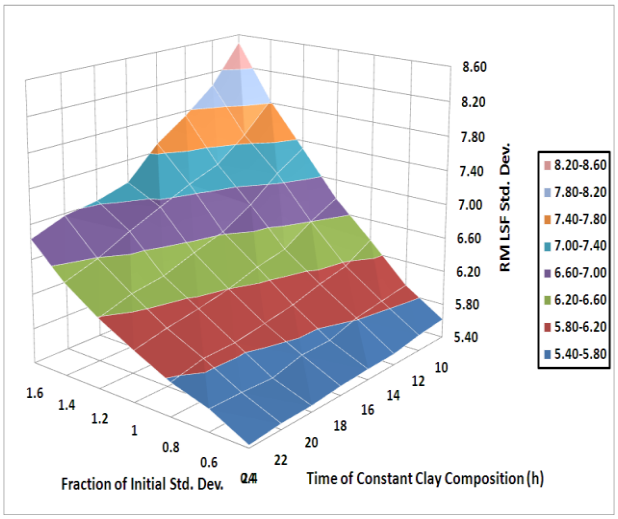


Figure 7. LSF standard deviation in RM outlet as function of the clays' variance.

From Figure 7 the extremely strong effect of the clays' stability on the raw meal homogeneity is verified. From the other side the time period that the mill is fed with constant material is not negligible at all. For the same long term variance of the clay, if the volumes of constant quality are larger, then the raw meal variance is lower. According to the simulation results, the variance of LSF in RM outlet for $s_{ox}=1.6 \cdot s_{ox,Init}$ and $T_{cc}$=24h is around equal with the one obtained for $s_{ox}=s_{ox,Init}$ and $T_{cc}$=10h.

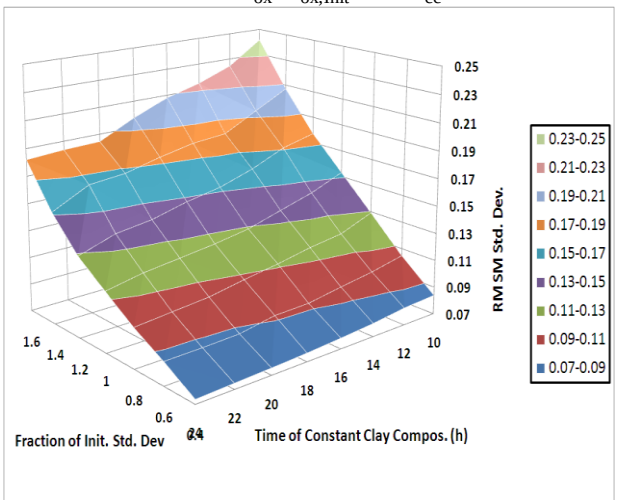


Figure 8. SM standard deviation in RM outlet as function of the clays' variance.

Similar results are also observed in Figure 8. The former remark indicates the high value of a pre-homogenizing system. The function between LSF standard deviation in the kiln feed and clays' variance is demonstrated in Figure 9. The conclusions extracted from Figures 7, 8 are soundly confirmed.

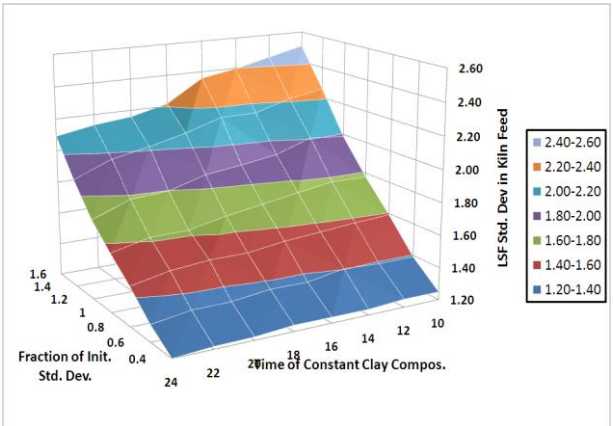


Figure 9. LSF standard deviation in kiln feed as function of the clays' variance.

## 3.2 Uncertainty of the Raw Mill Time Constants

The time constants $T_0$ and delay times $t_d$ of the two dynamics between the modules and RM feeders are presented in Table 3. Their uncertainty is also referred, which mainly is a function of the RM operating settings, i.e. RM feed flow rate, circulating load, separator speed and air flow rate. Normally as more stable are these parameters; lower is the uncertainty of the system time constants. To simulate the effect of $T_0$ and $t_d$ uncertainty on the raw meal variance the steps presented in section 3.1 are implemented: In equation (15) the oxides standard deviation is replaced by the $T_0$ and $t_d$ one. In Table 3 the time period with constant dynamics is between 8 and 20 hours resulting in an average period $T_{cd}$= 14 ± 6 hours. This period is varied from 10 ± 6 to 18 ± 6 hours with a step of 4 hours. The standard deviation of LSF in RM outlet is correlated with the time period $T_{cd}$ and the standard deviations of $T_0$ and $t_d$, considered as fractions of the ones shown in Table 3. The results are shown in Figure 10.

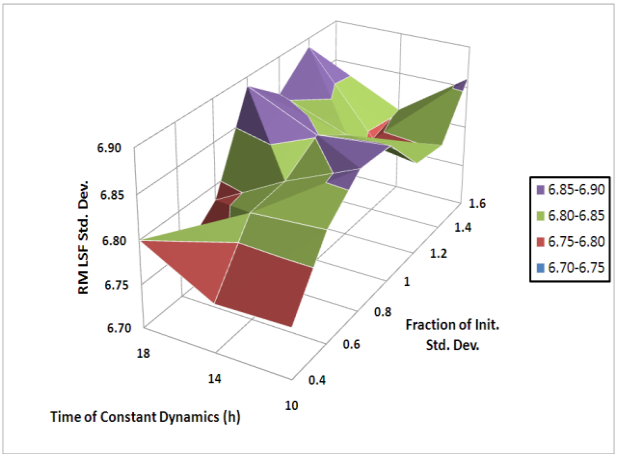


Figure 10. LSF standard deviation in RM outlet as function of the RM dynamics variance.

As it can be observed from this Figure, practically there is not any trend between LSF variance and parameters investigated. Consequently the studied range of dynamics variance while it is expected to have effect to the product fineness, it has not any noticeable impact on the modules variance. Thus, after the RM start up and if the feeders run normally, the raw meal shall be sampled by applying the routine sampling period, independently if the circulating load reached the operating point or not.

## 3.3 Active Mixing Volumes of Homo and Stock Silos

The process simulator is applied to examine the effect of the raw meal volumes actively participating in the mixing on the raw meal quality. To mention that the homo and stock parameters indicated in Table 3 are characterized from high uncertainty degree. The value of the active volume of the homo silo is mainly determined by the operation of the funs performing the stirring. As to the stock silo and for a given level of filing degree, the active material volume is defined by the existing dead stock and the way of the extraction from the silo's bottom.

To investigate the impact of the active material contained to each silo on the raw meal homogeneity the simulation is applied with the subsequent steps.

(a) The active mass of the homo is altered from 250 to 500 tn with a step of 50 tn.
(b) The exponent of the equation describing the time constant of the stock silo, $T_{Silo}$, is altered from -0.5 to -0.7 with a step of -0.1.
(c) For the above parameters the same uncertainties referred in Table 3 are utilized.
(d) The RM starts when the stock silo empty meters reach the five meters and stops when the meters are less or equal of three meters.

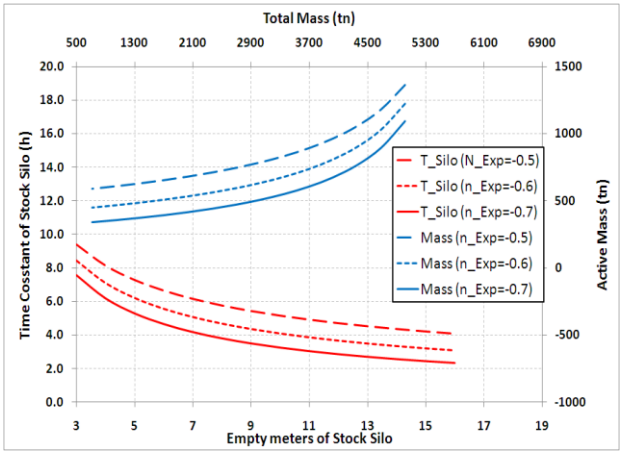


Figure 11. Stock silo time constant as function of the empty meters for various $n_{exp}$.

The function between $T_{Silo}$ and silo empty meters for the various exponents $n_{exp}$ chosen is shown in Figure 11. In the same Figure the active volume as function of the total mass of the raw meal inside the silo is depicted. Remind that the curves with $n_{Exp}$=-0.6 are obtained by adapting the model to industrial data. Because the flow in the stock silo is of funnel type only a 30% to 50% of the total mass participates to the mixing process.

The LSF standard deviation in the homo outlet as function of the homo active volume is presented in Figure 12.

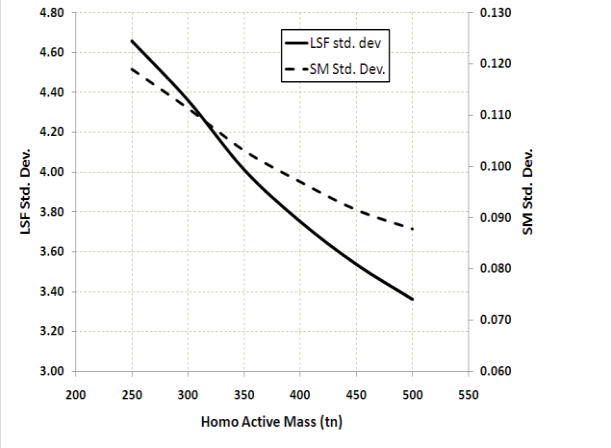


Figure 12. LSF and SM standard deviations in the homo outlet as function of the active silo volume.

From this Figure becomes clear that the homo active volume is a critical process parameter influencing the raw meal homogeneity. The maximization of this volume is obtained by the adequate fluidization of the material from the air produced with the respective blowers. The LSF and SM variances in the raw meal feeding the kiln are depicted in Figures 13 and 14.

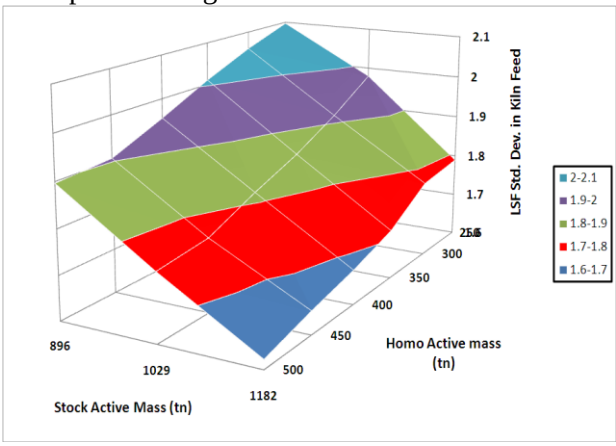


Figure 13. LSF standard deviation in the kiln feed as function of homo and stock active volumes.

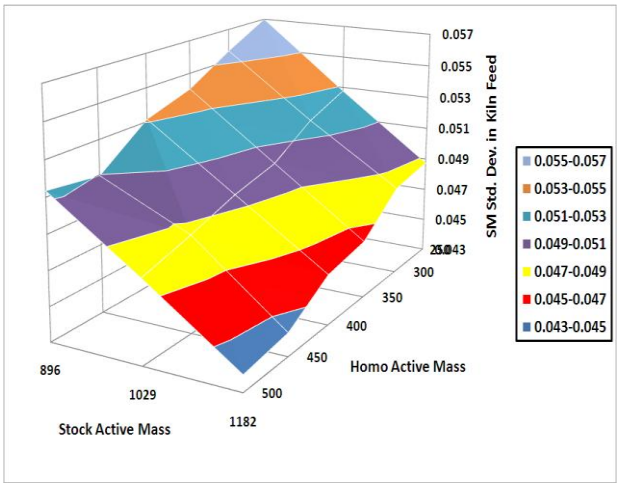


Figure 14. SM standard deviation in the kiln feed as function of homo and stock active volumes.

A bilinear function between the modules' standard deviation and silos' active volume appears, described from the equations:

$$s_{LSF} = 3.181 - 0.099 \cdot \frac{V_s}{100} - 0.083 \frac{V_H}{100} \qquad (16)$$

$$s_{SM} = 0.0851 - 2.59 \cdot 10^{-3} \cdot \frac{V_s}{100} - 2.19 \cdot 10^{-3} \cdot \frac{V_H}{100} \qquad (17)$$

Where $V_s$ and $V_H$ the volumes of active raw meal in stock and homo silo respectively expressed in tons. As it can be seen from the slops, the impact of 100 additional tons in stock and homo silos on the modules variance is around equivalent. Consequently the stock silo contributes significantly in raw meal mixing. The possible dead storage and the way of the extraction from the silo's bottom shall always be taken under consideration. Equations (16), (17) can be used as a tool to investigate the silos' behavior.

### 3.4 Filling Degree of the Stock Silo

In all the simulations applied till now it is considered that RM starts to grind when the stock empty meters are more than five and stops when they are less than three. Therefore fours meters are supposed as average. In the subsequent simulations the average empty meters are varied by keeping always a margin of ±1 m. The results are demonstrated in Figure 15.

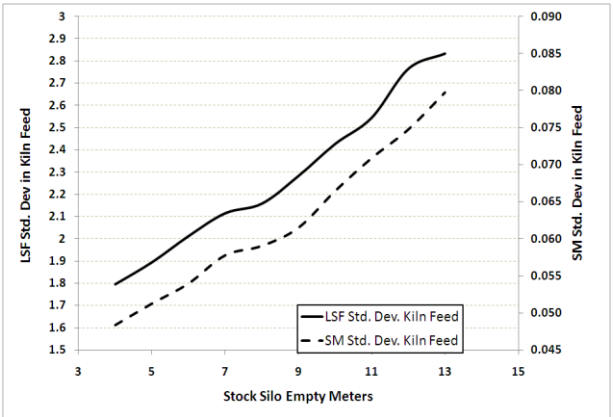


Figure 15. LSF and SM standard deviations in the kiln feed as function of stock empty meters.

The strong effect of the stock silo filling degree on the raw meal homogeneity fed to the kiln becomes apparent from the plots shown in Figure 15. As Johansen et al. clearly declare in [12] "In large, continuously operating raw meal silos, keep the silos full to maintain effective blending".

### 3.5 Measuring Time and Sampling Period

The delay time between raw meal sampling and feed-in of the new set points to the weight scales normally has an effect to the system response and the resulting regulation. To simulate the above two approaches are implemented:

- The data of Tables 2 and 3 are considered and a clay average analysis providing $K_g$=2.9 between limestone feeder and LSF.
- The measuring time is permitted to vary from 10 min to 30 min. The sampling period is always kept equal to 1 hour.

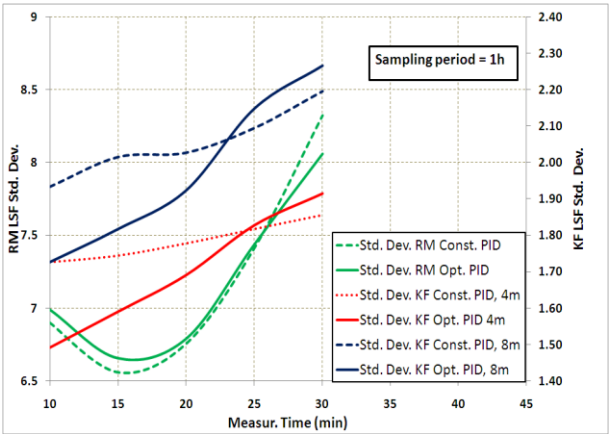


Figure 16. LSF standard deviations in the RM outlet and kiln feed as function of measuring time.

- In the first approach, for $t_M$=20 min, an LSF controller is selected with $M_s$=1.5 and $k_d$=0.08. In the second one for each $t_M$, MIGO technique is applied for $M_s$=1.5 and $k_d$ from 0 to $k_{d,Max}$.
- The procedure is applied twice: For average empty meters of the storage silo 4±1 m and 8±1 m.
- The LSF variance in RM outlet and kiln feed is computed.

The functions between these standard deviations and measuring time are plotted in Figure 16. In the case of MIGO application for each $t_M$, the minimum standard deviations is always obtained with $k_{d,Max}$.

Based on the results shown in Figure 16, the following remarks can be done.

- For constant PID coefficients, corresponding to the optimum controller for $t_M$=20 min, as $t_M$ increases, the same occurs for the both standard deviations.
- The same results are observed when optimum controllers are assumed parameterized according to $t_M$ value.
- The inclination of the correlation between $t_M$ and the variance of LSF in the kiln feed is noticeably higher in the latter case compared with the former one.
- The standard deviation in RM passes from a minimum as $t_M$ increases, probably because the controller is not optimum for $t_M$=10 min and $M_s$=1.5
- The minimization and stability of $t_M$ lead to a more effective tuning of the controller, resulting in a lower variance in the raw meal fed to the kiln. Consequently the automatic transfer of the sample to the XRF installation as well as the direct transfer of the controller's results to the weight scales can offer a substantial increase of the homogeneity of the material introduced to the kiln.

The time interval involving sampling of the raw meal, preparation and analysis, calculation of the feeders' new set points and transfer of these results to the scales is defined as measuring time $t_M$. The sampling period $T_s$ shall be higher than $t_M$ and depends also on the system time constants. To determine an optimum sampling period the total workload of the laboratory shall be taken into account as well as the cost of each analysis. To investigate the impact of the sampling period to the raw meal homogeneity for the installation under consideration the data shown in Table 4 are utilized. The remaining data are the ones utilized already in this section.

Table 4. $T_s$ and $t_M$ data

| $T_s$ (hours) | 2/3 | 1 | 2 |
|---|---|---|---|
| $t_M$ (minutes) | 15 | 20 | 20 |
| Stock silo average empty meters | | | |
| 4 | | 8 | |

For each $T_s$ and $t_M$, MIGO method is applied. The simulation results are presented in Table 5 and correspond to the PID controller providing minimum variance in RM outlet. For the three sampling periods the optimum PID settings are found for $M_s$=1.5.

Table 5. Impact of the $T_s$ on the raw meal variance

| $T_s$ (hours) | 2/3 | 1 | 2 |
|---|---|---|---|
| $t_M$ (minutes) | 15 | 20 | 20 |
| RM LSF Std. Dev | 7.04 | 6.77 | 8.45 |
| Empty Meters | KF LSF Std. Dev. | | |
| 4 | 1.64 | 1.69 | 2.47 |
| 8 | 1.89 | 1.92 | 2.79 |

From these results it is derived that the doubling of $T_s$, from one to two hours, causes a severe deterioration of the LSF standard deviation both in mill outlet and kiln feed, in spite that an optimum controller is selected. On the other side the decrease of $T_s$ by 33%, from 1 hour to 40 minutes, does not result in a substantial improvement of the raw meal quality, regardless of the 50% increase of the number of analysis. The above wrong selection shall be connected with the fact that for the given system and $T_s$=40 min, $T_s \leq t_M + t_d$.

# 4 Spot sampling in Raw Mill Outlet

## 4.1 PID Tuning and Comparison with Average Sampling

Due to the variance of the raw materials' composition, typically the sampling in RM outlet is performed via a sampling device which:

- During the sampling period continuously or in small time intervals accumulates raw meal specimens.
- When the sampling time arrives, it mixes them.
- Then a part of the total raw meal is extracted from the sampling device and transferred to the laboratory manually or automatically.
- The above constitutes the average sample, the analysis of which is fed to the PID controller.

In the case of inappropriate operation of some part of this device, the quality control department is obliged to take spot samples in order to regulate the raw meal quality up to the moment the sampling installation will be repaired. Furthermore there are cases of missing spare parts. Thus the spot sampling period is extended.

To investigate the effect of the spot sampling on the raw meal quality, the simulator is applied as follows:

- In the end of each sampling period, a spot sample is taken.
- The regulation is based on the analysis of this sample.
- Two cases of PID parameters are considered: In the first case the PID operates with the tuning performed using the average sample. In the second one, the transfer function $G_s$ shown in Figure 2 is omitted and new PID tuning is performed, based exclusively on the spot sampling.

The PID parameters of the latter tuning differ significantly from the ones computed when $G_s$ is a part of the process. The $k_p$ and $k_i$ values as function of $k_d$ are depicted in Figure 17 for $M_s$=1.5.

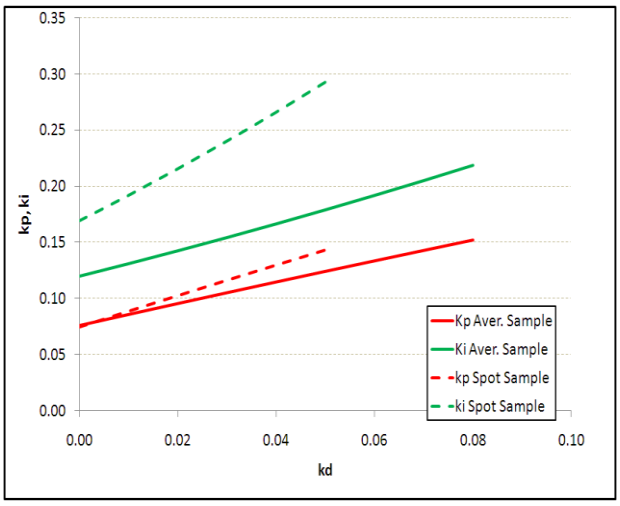


Figure 17. PID coefficients for average and spot sampling.

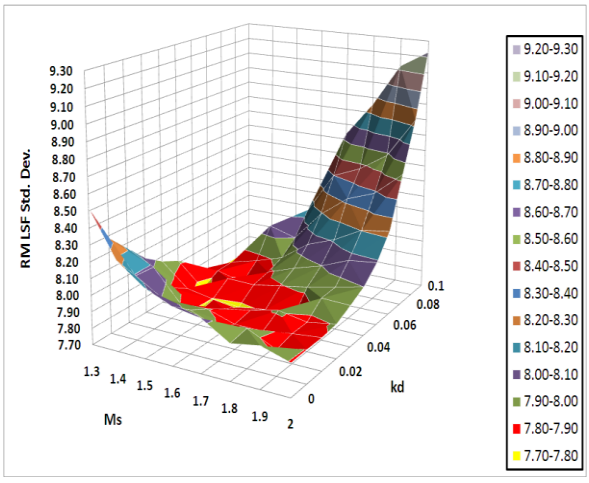


Figure 18. LSF standard deviation in RM outlet

The simulator is implemented using the data of the tables 2 and 3. Initially the tuning based on the

average sampling is applied. The LSF and SM standard deviations as function of PID parameters are shown in Figures 18 and 19 respectively. The same results for average sampling are depicted in Figures 20, 21

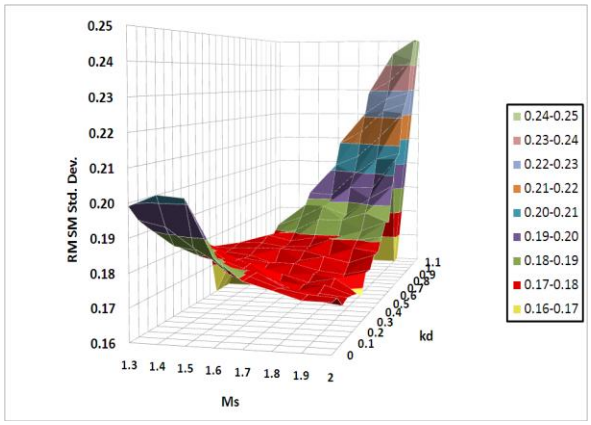


Figure 19. SM standard deviation in RM outlet

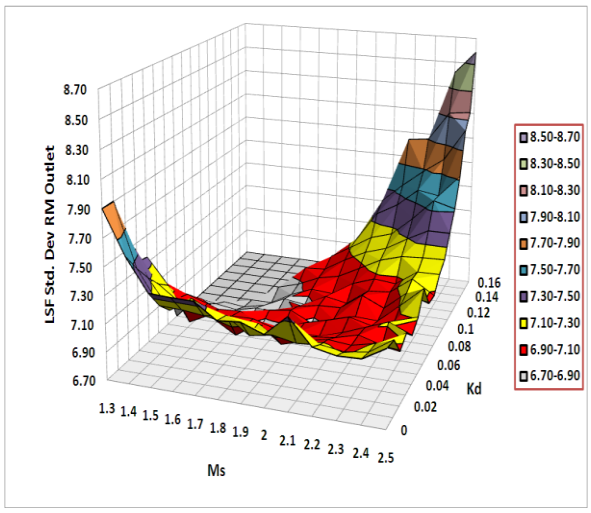


Figure 20. LSF standard deviation in RM outlet. Average sampling.

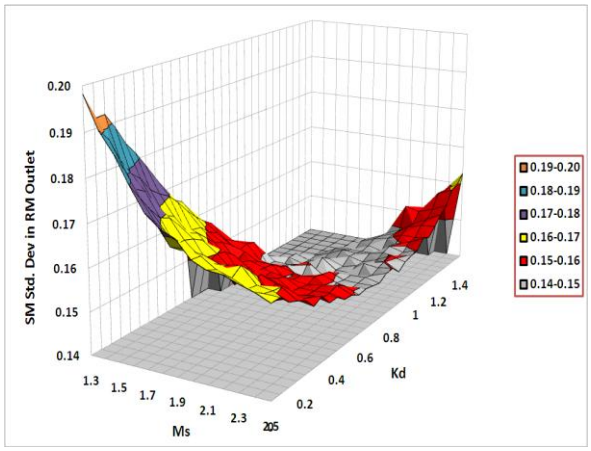


Figure 21. SM standard deviation in RM outlet. Average sampling.

From the comparison of the results of Figures 18, 19 with the ones of Figures 20, 21 it is derived that the regulation with spot sampling every $T_s$ period leads to a remarkable deterioration of the raw meal homogeneity in RM outlet. While for average sampling and for an optimum $M_s$, the minimum variance appears in the maximum $k_d$ values, for spot sampling the optimum $k_d$ is moved to lower values.

The tuning based on spot sampling is also implemented as to LSF regulation. The LSF standard deviation in RM exit as function of the PID parameters is shown in Figure 22. The results are not significantly different from those shown in Figure 18. Therefore the second tuning does not provide a better LSF variance comparing with the first one.

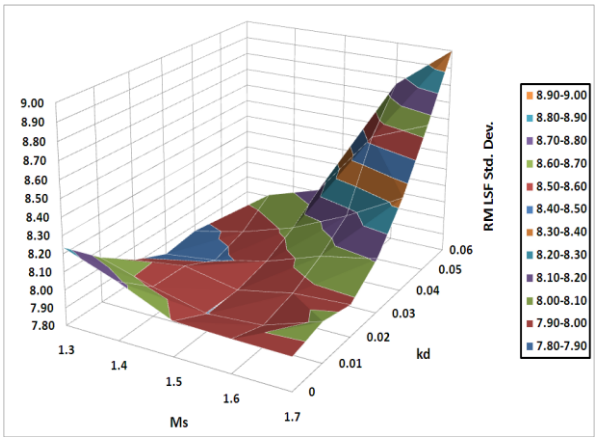


Figure 22. LSF standard deviation in RM outlet.

As a conclusion, in the case of regulation with spot sampling every $T_s$ time interval, the controller parameters extracted from the average sampling can be applied, but a $k_d$ on the middle of the $[0, k_{d,Max}]$ interval shall be chosen, to derive the minimum possible variance.

## 4.2 Differentiation of the Sampling and Measuring Frequencies

In the case of spot sampling and simultaneous measurement, the effectiveness of the remedial action to tune the PID by placing a lower $k_d$ controller is not strong enough as indicated in section 4.1. To search if a noticeable recuperation of the raw meal homogeneity can be achieved despite the spot sampling, another strategy is selected:

- The measuring period remains the initial sampling period $T_{s,}$ but within this time interval $N_{Spot}$ consecutive samples are taken with period $T_{Spot}=T_s / N_{Spot}$.
- In the end of $T_s$ the $N_{Spot}$ samples are mixed and measured.

- In this way the average sampling is simulated in some way.
- The analysis of the mixed sample is fed back to the PID controllers and the new feeders' settings are defined and put in operation.

This sampling and control strategy is simulated for $T_s$=60 min and $T_{Spot}$=30, 20, 15, 10 min. The simulation is applied for all the PID controllers parameterized with Ms=1.4, 1.5, 1.6 and average sampling. The LSF standard deviation results in RM outlet are compared with the ones of average and spot sampling every hour followed by measurement and indicated in Figures 23, 24, 25. The subsequent remarks can be made according to these results.

- The decrease of the spot sampling period and the formation of an average sample composed from the $N_{Spot}$ samples contribute to a decrease of the RM variance.
- The minimum $T_{spot}$ depends on the availability of the existing human resources.
- For the three investigated $M_s$ cases, a PID controller with low $k_d$ value provides the minimum LSF standard deviation.

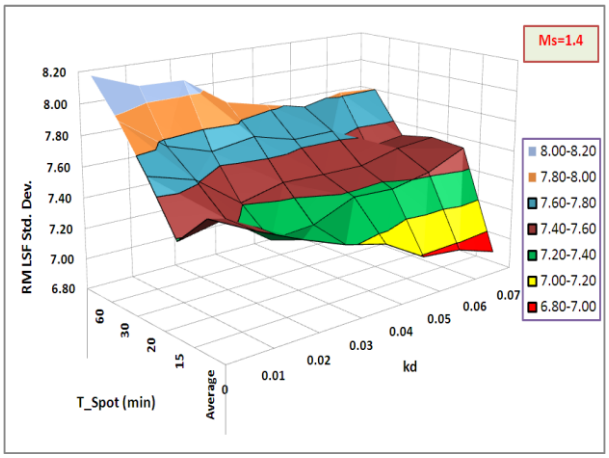


Figure 23. RM LSF std. dev as function of $T_{Spot}$ for $M_s$=1.4.

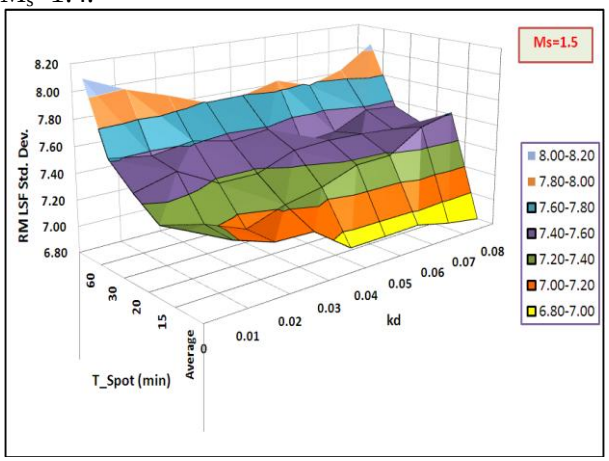


Figure 24. RM LSF std. dev as function of $T_{Spot}$ for $M_s$=1.5.

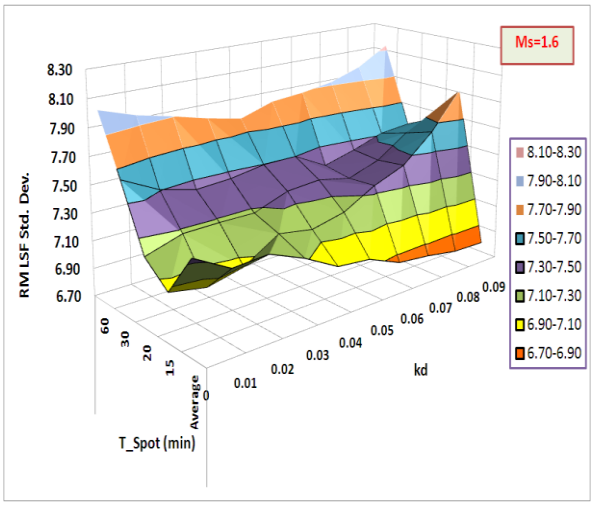


Figure 25. RM LSF std. dev as function of $T_{Spot}$ for $M_s$=1.6.

- The minimum LSF standard deviations $s_{Spot}$ for $T_{spot}$=10, 20, 30, 60 min and the one for average sampling every $T_s$=60 min $s_{Aver}$ are shown in Table 6. In the same Table the ratio $s_{Spot}/s_{Aver}$ is also presented.

Therefore the increase of the spot sampling frequency and the formation of a mixed sample every $T_s$ period can partially compensate the worsening of the raw meal homogeneity due to the absence of average sample extracted regularly from the sampling apparatus. The above results in the subsequent practical rule: For $T_s$=1h, a doubling of the sampling frequency derives an LSF standard deviation ~10% worse than the achieved with the average sampling. If it is possible to have a multiplication of the sampling frequency at four times, then the raw meal standard deviation becomes only 5% higher than the minimum one.

Table 6. Optimum Std. Dev of LSF in RM outlet as function of $T_{Spot}$

| | $M_s$ | | |
|---|---|---|---|
| | 1.4 | 1.5 | 1.6 |
| $T_{Spot}$ | $s_{Spot}$ | | |
| 60 | 8.09 | 7.87 | 7.78 |
| 30 | 7.47 | 7.42 | 7.37 |
| 20 | 7.41 | 7.37 | 7.20 |
| 15 | 7.25 | 7.12 | 7.05 |
| | $s_{Aver}$ | | |
| Average | 6.87 | 6.80 | 6.77 |
| | $s_{Spot}$ / $s_{Aver}$ | | |
| 60 | 1.18 | 1.16 | 1.15 |
| 30 | 1.09 | 1.09 | 1.09 |
| 20 | 1.08 | 1.08 | 1.06 |
| 15 | 1.05 | 1.05 | 1.04 |

# 5 Conclusions

Based on a dynamical model of the raw materials blending in closed circuit ball mill, two PID controllers were parameterized by applying the M-constrained integral gain optimization technique to the specific conditions of raw meal production and quality control. The settings of the limestone and additive weight feeders constitute the two control variables. As process variables the Lime Saturation Factor and the Silica Modulus are chosen. The simulation developed in [3] is applied to investigate the effect of the process parameters on the raw meal homogeneity.

The variance of the raw materials composition as well as the time period that the composition remains constant, have a strong impact on the raw meal variance both in RM outlet and kiln feed. Consequently a good pre-homogenizing system can contribute to quality improvement. The volume of the material contained in the homo and stock silos, participating actively in the mixing, has a noticeable effect on the variance of the product. Successful design and correct operation of air flow rate can achieve sufficient fluidization and dispersion of the material. The good filling degree of the stock silo has also a positive impact on the material mixing. An optimum PID controller, enhances the mixing ratio of the silos, by creating thin layers of material and facilitating the mixing.

The simulation is also implemented for different sampling periods $T_s$. For the given system a doubling of $T_s$ results in a severe deterioration of the LSF standard deviation both in mill outlet and kiln feed, despite the selection of an optimum controller. Sampling period should remain larger than the total of measuring and delay times. The minimization of the measuring time can lead to a more effective tuning of the controller. The previous results are based on the assumption of an average sample accumulated during $T_s$ via a sampling device.

The case of spot sampling is also studied. For the given variance of the raw materials and the same $T_s$, a remarkable worsening of the raw meal homogeneity appears. A small recuperation can be achieved by tuning the controller at lower $k_d$ values. An increase of the sampling frequency and formation of a mixed sample every $T_s$ can partially counterbalance the worsening of the raw meal stability. PID tuning based on average sampling is proving adequate in this case.

Consequently, it can be concluded that the developed simulator, not only can be applied to find the optimum PID controller among the sets satisfying certain robustness criteria, but also to determine optimum conditions of the process parameters.

*References:*


[1] Lee, F.M., The Chemistry of Cement and Concrete,*3rd ed. Chemical Publishing Company, Inc.*, New York, 1971, pp. 164-165, 171-174.

[2] Tsamatsoulis, D., Development and Application of a Cement Raw Meal Controller, *Ind. Eng. Chem. Res.*, Vol. 44, 2005, pp. 7164-7174.

[3] Tsamatsoulis, D., Effective Optimization of the Control System for Cement Raw Meal Mixing Process: PID Tuning Based on Loop Shaping and Process Simulators, accepted for publication in *WSEAS Transactions on Systems and Control*.

[4] Ozsoy, C. Kural, A. Baykara, C. , Modeling of the raw mixing process in cement industry, *Proceedings of 8th IEEE International Conference on Emerging Technologies and Factory Automation*, 2001, Vol. 1, pp. 475-482.

[5] Kural, A., Özsoy, C., Identification and control of the raw material blending process in cement industry, *International Journal of Adaptive Control and Signal Processing*, Vol. 18, 2004, pp. 427-442.

[6] Keviczky, L., Hetthéssy, J., Hilger, M. and Kolostori, J., Self-tuning adaptive control of cement raw material blending, *Automatica*, Vol. 14, 1978, pp.525-532.

[7] Banyasz, C. Keviczky, L. Vajk, I. A novel adaptive control system for raw material blending process, *Control Systems Magazine*, Vol. 23, 2003, pp. 87-96.

[8] Tsamatsoulis, D., Modeling of Raw Material Mixing Process in Raw Meal Grinding Installations, *WSEAS Transactions on Systems and Control*, Vol. 5, 2010, pp. 779-791.

[9] Astrom, K., Hagglund, T., Advanced PID Control, *Research Triangle Park: Instrumentation, Systems and Automatic Society*, 2006.

[10] Bavdaz, G., Kocijan, J., Fuzzy controller for cement raw material blending, *Transactions of the Institute of Measurement and Control*, Vol. 29, 2007, pp. 17-34.

[11] Bagdasaryan, A., System Approach to Synthesis, Modeling and Control of Complex Dynamical Systems, *WSEAS Transactions on Systems and Control*, Vol. 4, 2009, pp. 77-87.

[12] Johansen, V.C., Hills, L.M., Miller, F.M., Stevenson, R.W., The importance of cement raw mix homogeneity, *Cement Americas*, 2003.